Hua, Pengmin; Wang, Haichao; Xie, Zichan; Lahdelma, Risto

District heating load patterns and short-term forecasting for buildings and city level

Published in:
Energy

DOI:
10.1016/j.energy.2023.129866

Published: 15/02/2024

Document Version
Publisher's PDF, also known as Version of record

Energy 289 (2024) 129866

Contents lists available at ScienceDirect

Energy

journal homepage: www.elsevier.com/locate/energy

District heating load patterns and short-term forecasting for buildings and city level

Pengmin Hua [a,*], Haichao Wang [a,c], Zichan Xie [a], Risto Lahdelma [a,b]

[a] *Department of Mathematics and Systems Analysis, Aalto University, School of Science, P.O. BOX 11100, Aalto, Finland*
[b] *Department of Mechanical Engineering, Aalto University, P.O. BOX 14100, FI-00076, Aalto, Finland*
[c] *Institute of Building Environment and Facility Engineering, Dalian University of Technology, Dalian, 116024, China*

A R T I C L E I N F O

Handling Editor: Henrik Lund

Keywords:
District heat load forecasting
Clustering method
City
Buildings
Multiple linear regression
Artificial neural networks

A B S T R A C T

District heating (DH) load forecasting for buildings and cities is essential for DH production planning and demand-side management. This study analyzes and compares the hourly DH load patterns for a city and five different types of buildings over an entire year. The various operating modes introduce nonlinear dependencies between the DH load and the outdoor temperature. We compare the prediction accuracies of different multiple linear regression (MLR) and artificial neural network (ANN) models. Without nonlinear dependencies, both ANN and MLR provide good, almost identical prediction accuracies. In the case of nonlinear dependencies, ANN is superior to MLR. However, the novel clustering method eliminates nonlinear dependencies and improves the accuracy of MLR on par with the ANN. ANN methods can automatically adapt to various nonlinearities. The advantage of combining MLR with the clustering method is that it is simpler than designing an ANN method, although manual work is required. In addition, MLR methods provide more insight into load patterns and how the load depends on various factors compared with 'black-box' ANN models. The developed methodology can be widely applied to building- and city-level load analyses and forecasting in different DH systems combined with or without domestic hot water consumption.

1. Introduction

1.1. Background

The energy crisis and environmental problems have become a global focus because highly developed economies are increasing energy demand. For example, the heating and cooling sector represents half of the energy consumption in the European Union (EU) [1,2]. In most EU countries, the annual heat demand in buildings is the largest, surpassing electricity and cooling demands [3]. Thus, there is an urgent need for energy savings during heating. In 2016, the Energy Efficiency Directive updated the binding measures for EU countries to set a new 30 % energy efficiency target for 2030 [4]. In temperate and cold climates, district heating (DH) provides a more cost-effective and sustainable solution for supplying heat to buildings in urban areas [5]. It is vital to implement low-carbon smart energy systems in countries with high heat demands [6,7]. However, DH is a large and complex system with time delays and multi-level coupling [8,9]. Operating according to customer requirements is challenging, and improper operation can lead to considerable degradation in energy efficiency. Thus, demand-side management (DSM) has become popular [10], and many researchers have proven that DSM is crucial for improving the flexibility of DH to balance supply with demand better and reduce energy consumption [11,12]. Forecasting the short-term future DH load in buildings and districts/cities is a vital component in the application of DSM to optimize energy use and consequently reduce greenhouse gas emissions [13].

1.2. Related research and research gaps

White-box and black-box methods are typical for predicting the heat demand of buildings and districts/cities [14,15]. For the white-box method, a forecasting model of a building is developed based on detailed physics equations. Building energy simulation software such as TRNSYS, EnergyPlus, IDA-ICE, and CARNOT are typical tools for building models and forecasting heat loads. Ascione et al. adopted TERMUS® and EnergyPlus to analyze the link between climatic stress and building heating performance using two residential buildings in Italy [16]. Magni et al. summarized the features of the mathematical models employed in several building energy simulation tools. They

* Corresponding author.
E-mail address: pengmin.hua@aalto.fi (P. Hua).

https://doi.org/10.1016/j.energy.2023.129866
Received 24 May 2023; Received in revised form 21 November 2023; Accepted 30 November 2023
Available online 6 December 2023

Nomenclature

Abbreviation

DSM	Demand-side management
DH	District heating
EU	European Union
SH	Space heating
DHW	Domestic hot water
MLR	Multiple linear regression
ANN	Artificial Neural Networks
ARIMA	Autoregressive integrated moving average model
SVM	Support vector machine
LSTM	Long short-term memory
RF	Random forest
FFNN	Feedforward neural networks
RMSE	Root mean squared error
AMAPE	Adapted mean absolute percentage error
pp	Percentage point

Symbols

A	Area, m^2
T_{in}	Indoor temperature, °C
T_{out}	Outdoor temperature, °C
T_{thres}	Threshold when heat demand stops depending on outdoor temperature, °C
h_{in}, h_{out}	The composite heat transfer coefficient, $W/(m^2{\cdot}K)$
δ	The thickness of the layer of walls or roofs, m
λ	The thermal conductivity, $W/(m^2{\cdot}K)$
ϕ	The heat transferred between indoor air and outdoor environment, W
U	The overall heat transfer coefficient, $W/(m^2{\cdot}K)$
$\dot{m}$	The mass flow rate of ventilation, kg/s
c	The heat capacity of indoor and outdoor air, J/(kg·K)
η	The heat recovery factor of ventilation
$\hat{y}$	The predicted heat loads, MW or kW
y	The real heat loads, MW or kW
$\bar{y}$	The average heat loads, MW or kW
β	The regression coefficient matrix
X	Input matrix
ε	Error in time t, MW or kW
d	The dummy variables

Subscript

i	The index of layers, and it is from 1 to n; n is the total number of layers of walls
t	The index of time (hour), from 1 to N

evaluated the computational cost of an office building to support users in selecting a fit-for-purpose simulation tool [17]. Scholars have employed theoretical analysis methods or combined the above tools to predict building heat loads. Ghedamsi et al. presented a bottom-up approach to forecast the energy consumption of residential buildings in Algeria [18]. Kristensen et al. demonstrated a hierarchical archetype modeling framework combined with bottom-up physics-based dynamic building energy modeling to forecast the heat load of Danish single-family houses [19].

With the development of intellectualization in DH and increased heat load measurements, black-box methods, known as data-driven models, have become popular [14]. This is because black-box methods predict the heat load based on measurement data without detailed information about the physical building properties. Statistical regression models, such as decision trees, multiple linear regression (MLR), autoregressive, and autoregressive integrated moving averages (ARIMA), are typical black-box methods used for heat forecasting in buildings and districts [20]. Fang et al. proposed several forecasting models based on MLR and seasonal ARIMA to forecast a city's heating demand [21]. Giulla et al. developed an MLR approach to forecast the building energy requirements for building stock in Italy, including heating and cooling [22]. Other typical black-box methods include machine learning or deep learning methods such as random forest (RF), artificial neural networks (ANN), support vector machines (SVM), and clustering methods. Depending on the structure of the ANN, it can be divided into different methods, such as feedforward neural networks (FFNN), convolutional neural networks, and long short-term memory (LSTM). Many researchers have used machine learning methods, deep learning methods, or a combination of these to forecast heat load [23,24]. Koschwitz et al. compared the performance between ε-SVM regression and two nonlinear autoregressive exogenous recurrent neural networks (NARX RNN) in monthly load predictions [25]. Potočnik et al. applied several machine learning methods for a city's heat load forecasting and proved that Gaussian process regression obtained the best forecasting results [26]. Xue et al. proposed an algorithm based on the attention LSTM to predict the heating load for a district containing residential buildings [27]. Bünning et al. introduced two forecast correction methods to reduce the variance in an ANN for heat forecasting without using ensemble methods [28]. Wei et al. compared the heating load forecasting performances of seven machine learning algorithms, such as extreme gradient boosting (XGBoost), supported vector regression (SVR), and multilayer perceptron (MLP). They proved that SVR, XGBoost, and LSTM were among the top three in terms of performance [29]. Lumbreras et al. proposed a clustering method, the Q-algorithm, for the heat load prediction of 42 buildings with different energy demand profiles in Estonia [30]. Runge et al. compared the performances of several machine learning methods in heat load forecasting for a district and concluded that the LSTM and XGBoost models outperformed other techniques [13]. Pachauri et al. proposed a weighted linear aggregation of Gaussian process regression and a least-squares boosted regression tree, known as WGPRLSB, for heat and cooling load forecasting of heating, ventilation, and air conditioning (HVAC) systems in residential buildings [31]. Shakeel et al. developed an improved Facebook-Prophet (FB-Prophet) model with additional positional encoding layers to forecast DH consumption [32]. Gong et al. developed a new framework based on Informer to forecast the DH load. They proved that the Informer-based forecasting model can achieve the most accurate and stable predictions [7]. Liu et al. compared deep reinforcement learning models with conventional supervised models for an office building with a ground-source heat pump [33]. Xu et al. proposed an optimized MLP to forecast the heating and cooling of buildings [34]. Table 1 lists the details of black-box methods adopted in mentioned references.

Previous research has shown promising results when applying white-box, black-box, or a combination of these methods for heat load forecasting in buildings and districts/cities. However, some aspects require further investigation.

(1) The white-box method has poor universality and reproducibility because it requires building parameters and expert experience to obtain good forecasting results. A suitable method for this case may not apply to other buildings or cities.
(2) Previous research using data-driven models mainly focused on improving prediction accuracy by developing more complex methods and neglecting the applicability of these methods. These methods require better reproducibility, and it is difficult to

Table 1
Details of black-box methods adopted in previous studies.

Ref.	Method	Forecasting purpose	Selected Features	Buildings/Districts
[21]	Seasonal ARIMA; MLR	DH for SH and DHW	Outdoor temperature; Wind speed; Social components; Past behaviors	City
[22]	TRNSYS; MLR	Cooling and heating	Heating degree days; Cooling degree days; External temperature; Opaque surface; Glazed surface; Shape factors; Internal gains	Nonresidential building
[25]	ε-SVM regression; NARX RNN	District heating and cooling	Occupancy; Outdoor temperature; Relative humidity; Dew point temperature; Wind direction; Wind velocity; Precipitation intensity and quantity	District (200 nonresidential buildings)
[26]	Gaussian process; Traditional forecasting methods	DH	Outdoor temperature; Solar irradiance; Relative humidity; Wind speed; Weekly cycle, Yearly cycle; Population behavior; Aggregation of hourly values into daily features	District (residential, commercial, and industrial buildings)
[27]	Attention LSTM	DH for SH	Weather forecast; Historical heat consumption; Outdoor temperature; Indoor temperature	District (residential buildings)
[28]	ANN; RC model; Regression-based methods	DH	Outdoor temperature; Historical heat load; Date data	Three office Buildings and a building for working and living
[29]	SVR; RF; MLP; XGBoost; CNN; LSTM; K-nearest neighbor regression	DH for SH	Historical heat; Meteorological data (Outdoor temperature; Relative humidity; Solar irradiation); Weather forecast data; Date-time data; Electricity meters	District (residential buildings)
[30]	Q-algorithm	DH for SH and DHW	Outdoor temperature; Global solar irradiance on a horizontal plane; Wind speed; Wind direction; Time factors	Buildings with different types
[13]	FFNN; CNN; RF; LSTM; XGBoost; SVM; Light gradient boosting models	DH for SH and DHW	Outdoor temperature; Solar radiation; Relative Humidity; Time index variables; Occupancy variable	District
[31]	WGPRLSB	Heat and cooling load of HVAC systems	Relative compactness; Surface area; Wall area; Roof area; Overall height; Orientation; Glazing area; Glazing area distribution	Residential buildings
[32]	FB-Prophet	DH	Outdoor temperature; Humidity; Wind speed; Wind direction; Cloudiness; Sea level atmospheric pressure; Collection of weather variables; Historical; Data-time	District (buildings with different types)
[7]	Informer	DH for SH	Time variables; Outdoor temperature; Humidity; Wind speed; Air quality index; Supply and return water temperature; Flow rate; DH regulation signal; Historical heat load	District (residential buildings)
[34]	MLP	Heating and cooling	Surface area; Wall area; Roof area; Relative compactness; Overall height; Orientation; Glazing area; Glazing area distribution	Residential buildings

generalize them to actual projects. This is because the design of this type of method relies heavily on the competence and experience of specific experts, such as in the determination of hyperparameters, which is difficult for engineers who are not majoring in machine learning to understand and apply. MLR and ANN (considered FFNN) are two simple and most intuitive black-box prediction methods [22]. The potential of these two prediction methods for heat load forecasting requires further exploration.

(3) Most previous studies have been more dependent on the data or algorithms to improve forecasting accuracy, ignoring customer energy consumption behaviors and their correlation [35]. The DH load patterns of buildings and districts/cities must be researched further to understand how buildings function and how the demand-side load develops to adopt suitable forecasting methods based on their patterns.

(4) Many of the cases in previous research only predict the heat load for space heating (SH); for example, in China [7,27,29], the DH is used only for SH, allowing the system to be shut down during the summer. In some countries, such as the Nordic countries [21] and Estonia [30], DH is also used to produce domestic hot water (DHW); therefore, the system must operate year-round. According to Ref. [36], a sustainable DH system must supply DHW to buildings in the future. Previous studies have separately developed forecasting methods for buildings [22,28,30,31,34] and districts/cities [7,13,21,25–27,29,32]. More general methods that can be applied simultaneously to building- and district/city-level DH load forecasting require further research.

1.3. Research novelty

To fill the abovementioned research gaps, this study aimed to develop a convenient, general, and practical method for forecasting DH loads containing SH and DHW at the building and city levels to support a flexible and precise DSM. The novelty of this study is as follows:

(1) Analyze the yearly heat load patterns of a major city and buildings of different types to identify the significant factors affecting heat load forecasting at building and city levels, considering the delay in heat exchange, daily and weekly rhythms, holidays, and seasons.

(2) General short-term DH load forecasting methods based on the MLR and ANN are proposed for building- and city-level DH load forecasting. These methods are suitable for DH systems with SH alone or with DHW production.

(3) Develop a novel clustering method that significantly improves the accuracy of MLR forecasts in the case of nonlinearities owing to multiple SH load patterns for buildings.

1.4. Applications of research

The proposed clustering method can be used to analyze the DH load patterns of a building and city' with or without DHW. In addition to improving the forecasting accuracy of the MLR of buildings with nonlinear dependencies, the clustering method can be applied to other aspects, such as designing optimal methods or strategies to realize the DSM. The proposed forecasting methods can be applied to both building- and city-level DH load forecasting for countries where the DH supplies only SH, such as China, and where the DH supplies both SH and DHW, such as Nordic Countries.

The remainder of this manuscript is as follows. Section 2 introduces the case study and analyzes the SH consumption and heat load patterns of a city and five buildings. Section 3 presents the methodology of the study. Section 4 analyzes DH load patterns and presents a novel clustering method for handling nonlinear dependencies. Section 5 defines the predictors and parameters of the forecasting models. Section 6 presents the computational results obtained by applying the forecasting models at the city and building levels. Finally, Section 7 concludes the paper.

2. Case introduction and space heating consumption

2.1. Case introduction

Helsinki, the capital of Finland, with a population of approximately 658,000 in 2021, has a large DH system. Approximately 92 % of the total space and DHW heating demand in Helsinki is covered by DH [37]. We study the DH load at the city level and for five different types of buildings: a Residential building, an Office building, a Hospital, a Mall, and an Adult education center. In Helsinki, residential buildings account for approximately 62 % of the DH heated floor space [38]. The Finnish Meteorological Institute provided the historical weather data [39]. The Helen Company provided the historical DH load for Helsinki [37]. The historical DH load for the Residential building was provided by an unnamed real estate management company, and for other buildings by Ref. [40]. Table 2 summarizes information about Helsinki and the other buildings.

Missing data and outliers are the two most common types of abnormal data in this study. The abnormal weather parameters and DH loads were corrected using valid parameters in the temporal vicinity. Tables 3 and 4 summarize the weather parameters and DH load.

Table 2
Information for a city and five buildings.

Type	Name	Description
City	Helsinki	Capital of Finland, 92 % of floor space is connected to DH.
Buildings	Office	Work from 8:00–9:00 to 16:00–17:00 on workdays, and rest on weekends and holidays.
	Hospital	Large hospital with 24/7 operation.
	Residential building	A large multi-floor, energy-efficient residential building built in 2017.
	Mall	07:30–23:00 from Mon. to Thur.; 07:30–04:00 on Fri.; 08:00–04:00 on Sat.; 10:00–04:00 on Sun.
	Adult education center	Both daytime and evening courses on workdays, mainly day-time courses on Saturdays.

2.2. Analysis of space heating consumption

The SH depends mainly on weather factors. Thus, we first analyze the SH consumption of a building. The heat exchange process between a building and the outdoor environment is shown in Fig. 1.

When the outdoor temperature is colder than the indoor temperature, the heat transfer from the indoor to the outdoor temperature is

$$\varphi = AU(T_{in} - T_{out}) + \dot{m}c(1-\eta)(T_{in} - T_{out}). \tag{1}$$

Here, A is the area of the building envelopes, U is the overall heat transfer coefficient for the building envelopes (combination of conductive, convective, and solar radiation heat transfer), $\dot{m}$ is the mass flow rate of ventilation, η is the heat recovery factor of ventilation, and c is the heat capacity of air.

Outdoor temperature is a critical factor that must be considered. Indoor structures (walls, floor, and ceiling) and other components, such as lights, personnel, and furniture, affect the indoor temperature by exchanging heat through a combination of convection, conduction, and radiation. Therefore, the indoor temperature is a critical factor [41].

Determining the U-value is challenging because it is affected by many factors, and each factor is coupled. Thus, we analyze the main factors affecting the U-value. Equation (2) shows the theoretical formula for calculating U-value [42,43].

$$U = \frac{1}{\frac{1}{h_{in}} + \sum_{i=1}^{n} \frac{\delta_i}{\lambda_i} + \frac{1}{h_{out}}} \tag{2}$$

where h_{in} is the composite heat transfer coefficient of indoor air and interior walls or roofs, W/(m^2·K); h_{out} is the composite heat transfer coefficient of the outdoor environment and exterior walls or roofs, W/(m^2·K); δ is the layer thickness of walls or roofs, m; λ is the thermal conductivity, W/(m^2·K); i is the index of layers ranging from 1 to n; and n is the total number of layers of walls or roofs.

From Equation (2), h_{in} consists of the convection and conduction heat exchanges between the indoor air and the inner face of the walls and radiation between different walls, closely related to the fluid types and properties. In addition, indoor air temperature and speed are critical factors affecting h_{in} (mainly affecting convection and conduction). In practice, the indoor air speed is low; hence, it was not considered when forecasting the heat loads. The heat exchange caused by radiation between different walls is smaller than convection and conduction and is difficult to calculate because of the heat exchange delay of indoor thermal objects. Therefore, we consider historical parameters (historical indoor air temperature and air speed) as important factors to describe h_{in}.

h_{out} consists of the convection and conduction heat exchanges between the outdoor air and the outer face of the walls and radiation between the outdoor environments. Outdoor temperature and wind speed are the two main factors that affect h_{out} caused by convection and conduction. Regarding the factors affecting h_{out} caused by radiation, only the heat exchange caused by solar radiation is considered. Considering the heat exchange delay of outdoor thermal objects, historical parameters (historical outdoor temperature, wind speed, and solar radiation) are also regarded as important factors. Other factors, such as wind direction and relative humidity, show minimal improvement in forecasting accuracy and can be considered negligible.

Some factors, such as the area of the building envelopes A and thermal conductivity λ of enclosure structures, are relatively fixed. This implies that these factors do not change once a building is completed. Furthermore, these factors affect the heat load of buildings based on Equation (2) but not the heat load change of the buildings. In other words, a change in the heat load of a building is caused by changes in factors such as a change in outdoor temperature. In addition, data-driven models consider the effects caused by these factors and learn rules using a training dataset to determine suitable structures or parameters for the forecast model.

Although many factors affect the U-value, it is difficult to identify all of them. Therefore, the primary factors must be selected. Based on the above analysis, factors such as indoor and outdoor air temperatures, wind speed, solar radiation, and historical parameters were determined to affect the U-value.

3. Methodology

We consider two types of forecasting models: MLR and ANN. Linear regression models work well when all dependencies are linear. Neural networks can handle nonlinear dependencies and automatically adapt to various situations.

3.1. Multiple linear regression

The MLR model is as follows:

$$\hat{y} = \beta X + \varepsilon. \tag{3}$$

Here, $\hat{y}$ is the predicted DH load; X is the input variable matrix; β is the vector of regression coefficients; and ε is the error vector. The regression model determines the regression coefficients to ensure $\varepsilon = \hat{y} - \beta X$ is as small as possible in the least squares sense, as shown in

Table 3
Information on weather parameters in 2020 and 2021.

Year	Outdoor temperature (°C)			Wind speed (m/s)			Solar radiation (W/m^2)		
	Min	Max	Average	Min	Max	Average	Min	Max	Average
2020	−8.9	28.9	8.4	0.0	15.1	4.8	−8.9	957.6	145.4
2021	−21.8	31.7	6.4	0.0	12.8	4.6	−7.2	943.6	134.6

Table 4
Information on the DH load of the city and five buildings.

Name	DH load (MW for city/kW for buildings)					
	2020			2021		
	Min	Max	Average	Min	Max	Average
Helsinki	178.8	1736.3	726.3	30.1	2422.6	853.0
Office building	10	400	151.2	10	630	183.2
Hospital	80	2420	885.3	60	3760	1032.4
Residential building	12	232	87.2	11	325	100.2
Mall	48	1198	472.0	31	1685	555.0
Adult education center	5	203	57.9	4	327	72.0

Equation (4).

$$\min \sum_{t=1}^{N} \varepsilon_t^2. \tag{4}$$

3.2. Artificial neural networks

A common method for modeling the intricate connections between inputs and outputs is the nonlinear statistical data modeling method known as ANN. The input, hidden, and output layers constitute the fundamental framework of an ANN. The neurons linking the input and output layers comprise the hidden layers. A basic ANN structure with two hidden layers is illustrated in Fig. 2.

The backpropagation (BP) algorithm employs ANN and has been widely used because of its powerful learning and generalization abilities [44].

3.3. Evaluation indicators

To evaluate the accuracy of the forecasting models, we use the coefficient of determination R^2, relative root mean squared error (RMSE %), and adapted mean absolute percentage error (AMAPE%) [21]. R^2 ranges from 0 to 1. Furthermore, the accuracy increases as R^2 approaches 1. The AMAPE% and RMSE% values are between 0 % and 100 %, with lower values indicating higher accuracy. With $\bar{y}$ equal to the average y_t, the indicators are defined as follows:

$$R^2 = 1 - \frac{\sum_{t=1}^{N} (y_t - \hat{y}_t)^2}{\sum_{t=1}^{N} (y_t - \bar{y})^2}, \tag{5}$$

$$RMSE\% = \frac{\sqrt{\left(\frac{1}{N}\sum_{t=1}^{N} (\hat{y}_t - y_t\right)^2}}{\bar{y}} \cdot 100\%, \tag{6}$$

$$AMAPE = \left(\frac{1}{N}\sum_{t=1}^{N} \frac{|\hat{y}_t - y_t|}{\bar{y}}\right) \cdot 100\%. \tag{7}$$

4. Analysis of district heating load patterns

4.1. District heating load patterns

In addition to weather parameters, SH depends on calendar cycles if the indoor temperature and ventilation rate are adjusted according to building use. DHW heating depends mostly on human behavior and is linked to yearly, weekly, and daily calendar cycles.

(1) The heating season occurs when DH is used for space and DHW heating. During this period, we referred to the following *winter*.
(2) During the non-heating season or *summer*, SH is mostly switched off, and DH is mainly used for DHW. The summer season may vary slightly from year to year and between different buildings; however, we assume that summer starts on May 16th and ends on September 15th, which is typical in Helsinki.

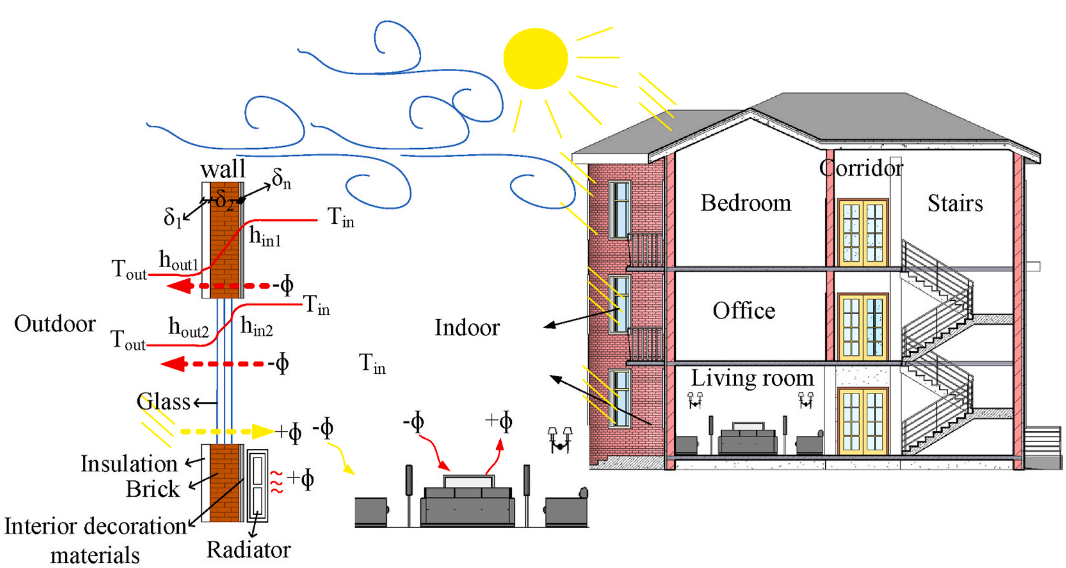

Fig. 1. Heat exchange process between the indoor and outdoor environments.

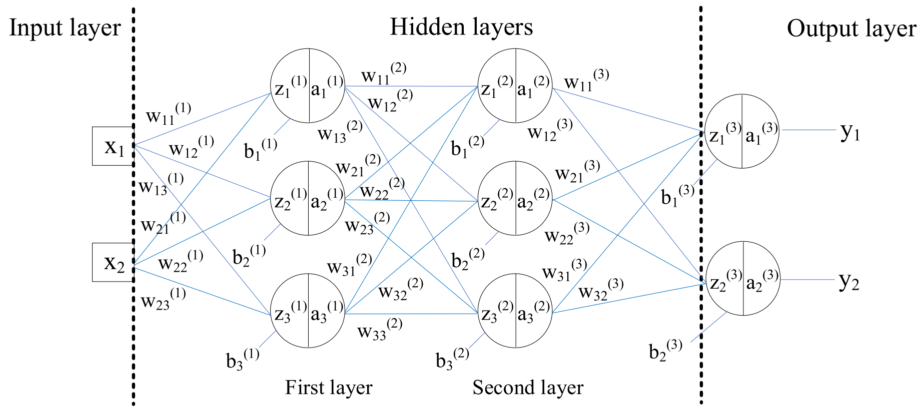

Fig. 2. Simple ANN structure.

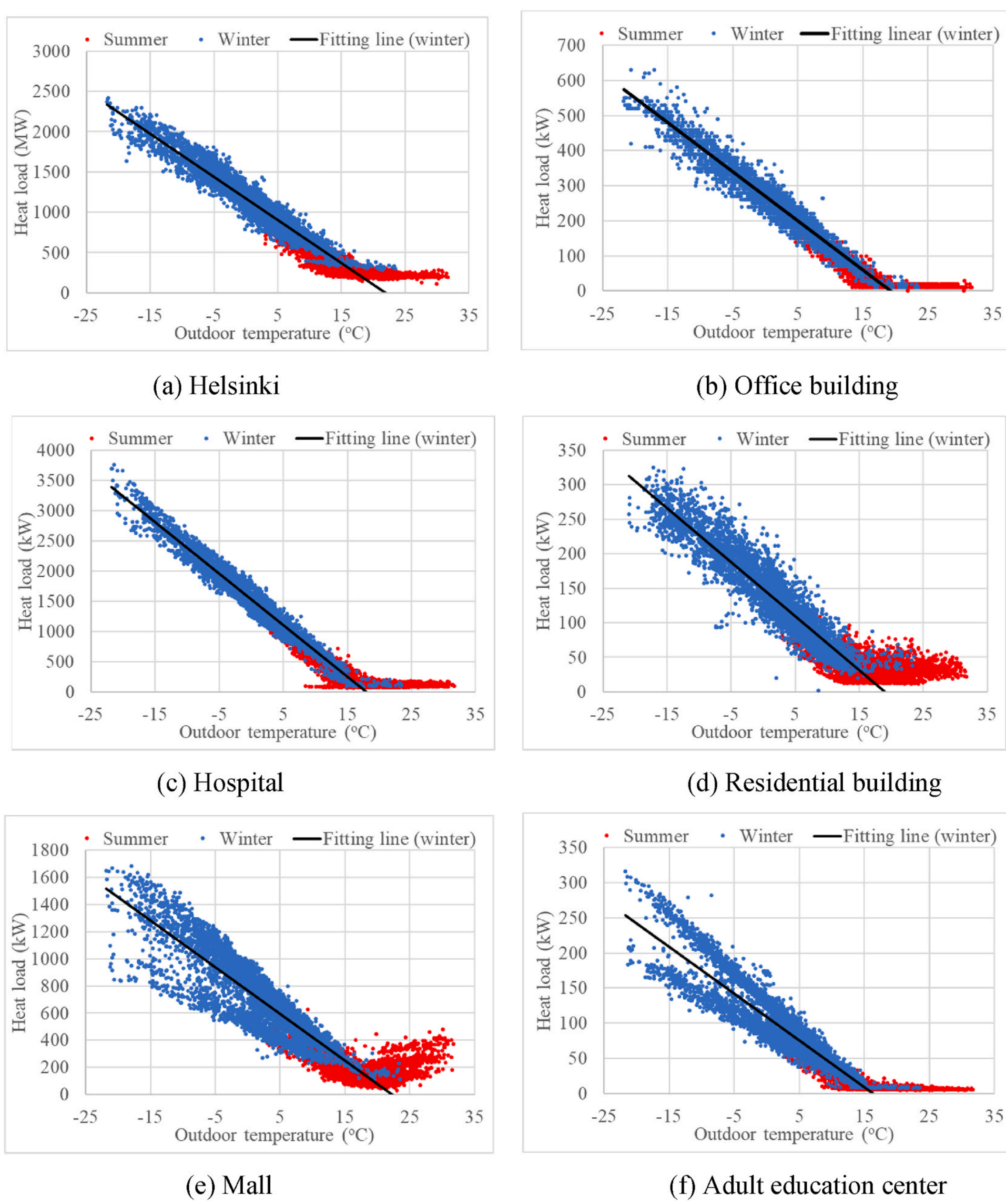

Fig. 3. DH load of Helsinki and various buildings in 2021.

Fig. 3 shows the hourly DH load in winter and summer for Helsinki and the five buildings as a function of the outdoor temperature in 2021. The regression line for the winter load is also included. The regression line provides a simple forecast of the winter DH load as a function of outdoor temperature. The hourly DH load depends strongly on the outdoor temperature, provided it is colder than approximately 17 °C. SH is switched off at warmer outdoor temperatures. This implies that the winter heat load nonlinearly depends on the outdoor temperature, with a bending point of 17 °C. In summer, the temperature dependency becomes much weaker because the SH is switched off, and the DHW heating load does not depend much on the outdoor temperature.

The load patterns for Helsinki, Residential building, Office building, and Hospital are similar and follow a simple regression forecast. Of these, the Residential building exhibits significant variation because it has high DHW consumption, which has a significant random variation owing to individual resident behavior. The Office building, Hospital, and Adult education center exhibit minimal DHW consumption. For the Mall and Adult education center, the load patterns do not follow the winter regression line. For these buildings, the DH loads are clustered around multiple lines with different slopes, indicating that other important factors affect the DH load.

4.2. Clustering method

This section develops a novel clustering method to identify and handle nonlinearities in winter DH loads owing to multiple load patterns for a building. The objective is to form clusters of hourly data such that, within each cluster, the dependency of the DH load on the weather (outdoor temperature) is close to linear. The clustering was performed in three phases.

(1) Fit a regression model to *winter* data.
(2) Divide the hourly data into *groups* based on how the average DH load differs from the regression model at different times of the day and on different weekdays.
(3) Fit a regression model for each *group* and form *clusters* with similar regression parameters.

Next, we apply the clustering method to the Mall and the Adult education center as examples.

In Phase 1, we use simple regression models with outdoor temperatures to predict the DH load, as presented in Section 4.1.

In Phase 2, we consider grouping according to different times of the day and weekdays, including national midweek holidays (whose DH load may be similar to nonworking days). Fig. 4 shows the average error between the simple regression line prediction and the actual hourly heat demand on different days and times of the day for the two buildings. A positive error indicates the actual heat demand is lower than the forecast, whereas a negative error implies the opposite. For example, the error was positive at night, indicating that the actual DH load was below the regression line shown in Fig. 3.

For the Mall, the daily pattern is similar for all days because the Mall operates every day. The small differences between 6:00 and 8:00 were because of the later opening times on weekends. The actual DH load was lower than the regression line forecast at night and higher between 9:00 and 21:00. A lower nighttime DH load is caused by smaller DHW consumption and a lower ventilation rate during off-hours. While a smaller DHW consumption shifts the DH load by a constant, a lower ventilation rate reduces the slope of the outdoor temperature dependency.

For the Adult education center, the DH load patterns from Monday to Friday were similar; however, for Saturday and Sunday, they differed. Heat demand depends on the programming of the heating and ventilation systems of the building. During nonworking hours, the ventilation rates are reduced, leading to a lower load and temperature-dependent factor. Surprisingly, the DH load on holidays was similar to that on working days. This indicates that the heating and ventilation system is not programmed to differentiate the midweek holidays from normal working days, including when the building is empty.

Based on Fig. 4, the hourly heat demand was divided into several groups. For the Mall, we grouped days into weekdays (Monday to Friday and holidays) and weekends (Saturday and Sunday). The weekday hours were divided into four intervals of 8–19, 20–0, 1–5, and 6–7. The weekend hours were divided into 9–19, 20–0, 1–4, and 5–8 intervals. For the adult education center, we grouped days into workdays, Saturdays, Sundays, and holidays. Workdays and holiday hours were divided into intervals of 8–22 and 23–7. Saturday hours were divided into 8–16 and 17–7 intervals. For Sundays, all the hours formed a single group.

In phase 3, we fit a linear regression model separately for each group and cluster the periods with similar regression parameters (slopes and intercepts of the regression lines). Table 5 lists the different periods and regression parameters for each group and cluster with similar regression parameters. We obtained four clusters from the winter data for the Mall and two from the Adult education center. Furthermore, considering the summer cluster, we obtained five clusters for the Mall and three for the

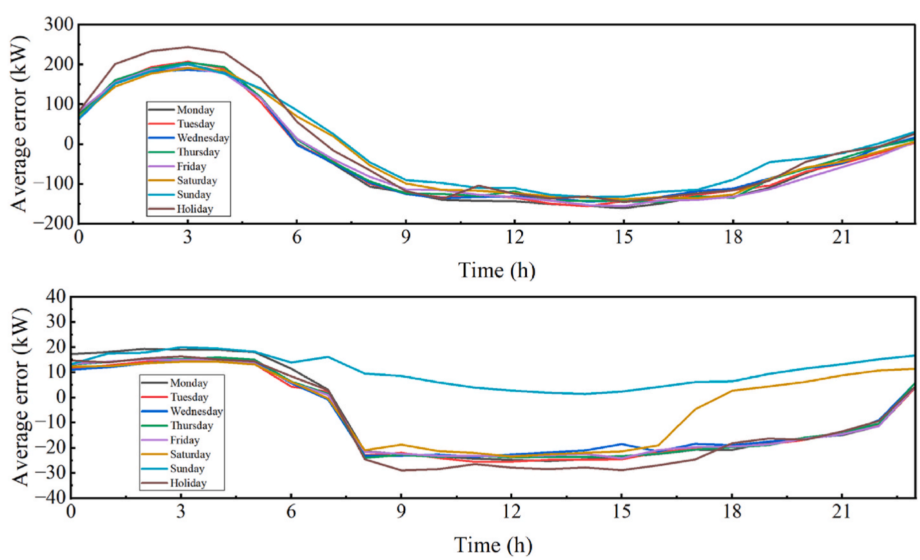

Fig. 4. Average error between the winter regression line forecast and the hourly heat demand for different days and times of the day. Top: Mall; Bottom: Adult education center.

Table 5
Groups and clustering of hourly DH load for Mall and Adult education center.

Mall				
Days groups	Hourly intervals	Slope (kW/°C)	Intercept (kW)	Cluster
Weekdays	8–19	−40.84	880.26	1
	20–0	−36.66	759.65	2
	1–5	−21.59	536.78	3
	6–7	−33.68	776.43	2
Weekends	9–19	−40.46	864.02	1
	20–0	−36.30	749.52	2
	1–4	−23.68	528.73	3
	5–8	−29.29	685.44	4
Adult education center				
Days groups	Hourly intervals	Slope	Intercept	Cluster
Weekdays	8–22	−8.38	130.53	1
	23–7	−5.52	91.99	2
Saturday	8–16	−8.21	130.83	1
	17–7	−5.58	92.40	2
Sunday	0–23	−5.08	84.66	2
Holiday	8–22	−8.00	125.81	1
	23–7	−5.42	92.65	2

Adult education center.

To illustrate the clusters, Fig. 5 presents the heat demand for the first cluster of the Mall, consisting of weekdays 8–19 and weekends 9–19. It is evident that the heat demand for both subgroups drawn with different colors is well centered around a single regression line. The other clusters show similar linear dependencies on the outdoor temperature.

In summary, the DH load patterns differ by city and building type. The load patterns depend on the season (*winter/summer*), weekday, and time of day. This is caused by the occupancy of the buildings and how the heating and ventilation systems are programmed to adjust the indoor temperature and ventilation rate.

5. Forecasting models

5.1. Predictors and sliding window

Based on the analysis discussed in the previous section, the main factors for the prediction model proposed in this study are determined. These factors apply to city- and building-level DH load forecasting.

(1) Weather parameters: outdoor temperature, solar radiation, and wind speed.

(2) Time parameters: season (winter/summer), daily rhythm (24 h), and weekly rhythm (7 days).

In addition, the indoor temperature is also an essential factor. In Finland, it generally ranges from 20 °C to 26 °C [21]. Because of the unavailability of the building's indoor temperature measurements, we assume a constant 20 °C. Hence, the indoor temperature can be ignored as a predictor.

We first divide the data into training and testing sets to apply the forecasting methods. We defined dummy variables (indicator variables) to represent seasonal, daily, and weekly rhythms in the prediction model [45]. For example, Table 6 presents the dummy variables for weekly rhythms. The holidays in the midweek are regarded as workdays for all buildings.

We use a 25-h sliding time window to forecast the hourly DH load. This means we use the weather parameters and rhythms in the past 24 h and the weather parameters and rhythms in the current hour to predict the load in the 25th hour. Subsequently, we move the sliding window to the next hour and repeat the above process, as shown in Fig. 6.

5.2. Parameters of forecasting models

To decrease the number of input variables for MLR, we use Akaike's Information Criterion to select the predictors. We then compare the three forecasting models based on MLR, as presented in Table 7. In the MLR models, model 2 indicates seasonal information, model 24 indicates daily rhythm, and model 7 indicates weekly rhythm.

Generally, when the outdoor temperature exceeds a threshold temperature T_{thres}, the dependency between the heat demand and outdoor temperature disappears. This makes the temperature dependence of the heat demand nonlinear. Because MLR does not adapt well to nonlinear dependencies, we use the minimum real temperature and T_{thres} to fit the MLR model. In Finland, $T_{thres} = 17$ °C is typically used for this purpose.

For the ANN, we use data from 2020 for training and validation and 2021 for testing. The proportions of the data for training and validation are 90 % and 10 %, respectively. Similar to the MLR models, we compare the three ANN models with different amounts of temporal information: season, daily rhythm, and weekly rhythm. The hyperparameters of the three ANN models are listed in Table 8.

6. Results

We applied six models based on MLR and ANN to a city and five

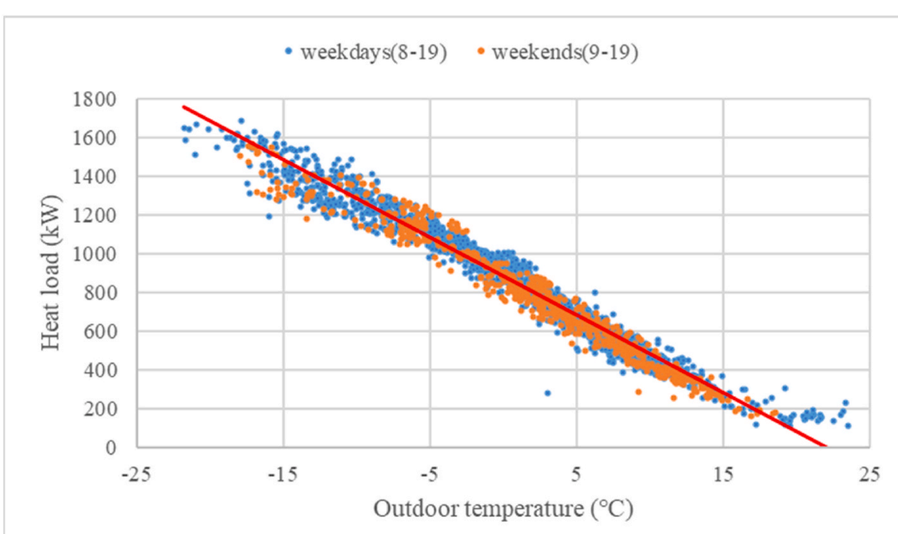

Fig. 5. Cluster 1 for the winter heat demand of the Mall consisting of weekdays 8–19 and weekends 9–19.

Table 6
Dummy variables for representing different days in a week [45].

Variables	$d_{1,t}$	$d_{2,t}$	$d_{3,t}$	$d_{4,t}$	$d_{5,t}$	$d_{6,t}$
Monday	1	0	0	0	0	0
Tuesday	0	1	0	0	0	0
Wednesday	0	0	1	0	0	0
Thursday	0	0	0	1	0	0
Friday	0	0	0	0	1	0
Saturday	0	0	0	0	0	1
Sunday	0	0	0	0	0	0

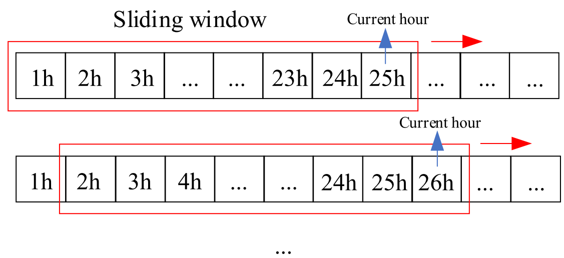

Fig. 6. Schematic diagram of sliding time window.

Table 7
Description of proposed models based on MLR.

Models	Predictors considered	Number of inputs
MLR_2	Historical and current outdoor temperature, wind speed, solar radiation, and seasons	25~40
MLR_2/24	Adding daily 24 h rhythm to MLR_2	
MLR_2/24/7	Adding weekly 7-day rhythm to MLR_2/24	

building types. The results are summarized in Table 9. The daily and weekly rhythms can improve the accuracy of the MLR and ANN models at the city level and for all buildings. Next, we analyzed and compared the DH load forecasting accuracy at the city and building levels.

6.1. DH load forecasting at city level

Based on Table 9, the MLR and ANN models performed well in DH load forecasting at the city level, with $R^2 > 0.97$. The ANN models exhibited slightly better forecasting accuracy than the MLR models, regardless of whether the rhythms were considered: AMAPE (7.81 %, 7.55 %, and 7.38 %) for MLR versus (7.37 %, 6.28 %, and 5.62 %) for ANN. Fig. 7 shows the DH load forecasting results of the city for a sample week in winter.

In Fig. 7, the DH load forecast without rhythms, marked in red, follows, on average, the real load using both MLR and ANN but fails to reach the peak and valley values. The models that added rhythms, marked in green and blue, slightly improved the forecasting accuracy. The MLR and ANN models with daily and weekly rhythms exhibited better forecasting accuracy at the city level in winter. The same conclusion applies to the DH load forecasting in summer.

6.2. DH load forecasting at building level

Based on Table 9, the ANN_2/24/7 model applies well to buildings of various types and produces the most accurate forecasting results at the building level compared to the other models, with each R^2 value higher than 0.93 and AMAPE below 10 %, except for the Residential building. Similar to the city level, for building DH load forecasting, adding daily and weekly rhythms to the MLR and ANN models improved the accuracy (Table 9). For the Office building, Hospital, and Residential building, the improvements owing to the introduction of a daily rhythm were minimal, with the AMAPE improving by less than 1.0 pp (percentage point). Adding daily rhythms to the Mall and Adult education center significantly improved forecasting accuracy. The AMAPE improved by 3.0 pp and 0.7 pp for the Mall and 2.0 pp and 1.8 pp for the Adult education center when applying MLR and ANN, respectively. Adding the weekly rhythm further improved the forecasting accuracy. For the Adult education center, the improvement of 1.3 pp and 3.3 pp (MLR vs. ANN) was significant; however, it was less than 0.4 pp for the other buildings. The results obtained in this study are consistent with those presented using the clustering method in Section 4.

MLR with daily and weekly rhythms can achieve good forecasting accuracy for the city and buildings, with a predominantly linear relationship between the hourly DH load and outdoor temperature. However, the MLR is less accurate for buildings with a weaker dependency between the hourly DH load and outdoor temperature. To better handle the nonlinearities owing to different winter load patterns for the Mall and Adult education center, we fit the MLR model with daily and weekly rhythms separately for the clusters of hourly demand formed in Section 4.2. Table 10 presents the forecasting accuracy of the clusters and combined forecasts. Cluster-based MLR significantly improves forecasting accuracy. Regarding AMAPE%, the accuracy of the cluster-based MLR is now identical to that of the best neural network model, ANN_2/24/7, for the Mall and approximately 1 pp worse for the Adult education center. Fig. 8 illustrates the forecasting results for the Adult education center using MLR_2/24/7, MLR_24/7 with three clusters, and ANN_2/24/7.

To summarize, MLR can provide forecasts with an accuracy comparable to that of ANN. However, in the case of nonlinearities for specific buildings, they must be identified, as described in Section 4, which may require manual work. The advantage of the ANN over the MLR is that the ANN model can adapt automatically to various nonlinearities and DH load patterns.

Table 8
Hyperparameters of ANN models.

Hyperparameters	ANN_2	ANN_2/24	ANN_2/24/7
Predictors considered	Historical and current outdoor temperature, indoor temperature, wind speed, solar radiation, and seasons	Adding daily rhythm based on ANN_2	Adding weekly rhythm based on ANN_2/24
Number of epochs	600–1200		
Batch size	64,128		
Optimization algorithms	Adam [46]		
Activation function	ReLU [47]		
Initial learning rate	$1e^{-5}$-$1e^{-2}$		
Regularization factor	$1e^{-5}$-$1e^{-1}$		
Number of hidden layers	1		
Number of neurons	100/64/1	675/256/1	825/256/1

Table 9
Evaluation indicators for DH load forecasting.

Name	Models	R^2	RMSE (%)	AMAPE (%)
City	MLR_2	0.972	10.24	7.81
	MLR_2/24	0.974	9.80	7.55
	MLR_2/24/7	0.976	9.55	7.38
	ANN_2	0.974	9.81	7.37
	ANN_2/24	0.982	8.26	6.28
	ANN_2/24/7	0.984	7.50	5.62
Office building	MLR_2	0.973	12.08	8.98
	MLR_2/24	0.975	11.60	8.55
	MLR_2/24/7	0.976	11.39	8.33
	ANN_2	0.976	11.28	7.87
	ANN_2/24	0.978	10.89	7.62
	ANN_2/24/7	0.978	10.87	7.64
Hospital	MLR_2	0.979	11.16	8.57
	MLR_2/24	0.980	10.81	8.36
	MLR_2/24/7	0.981	10.60	8.20
	ANN_2	0.985	9.55	7.23
	ANN_2/24	0.986	9.12	6.95
	ANN_2/24/7	0.986	9.04	6.89
Residential building	MLR_2	0.912	20.90	15.93
	MLR_2/24	0.923	19.53	14.93
	MLR_2/24/7	0.925	19.29	14.70
	ANN_2	0.932	18.37	13.77
	ANN_2/24	0.936	17.88	13.14
	ANN_2/24/7	0.938	17.48	13.09
Mall	MLR_2	0.876	22.26	15.99
	MLR_2/24	0.918	18.11	12.95
	MLR_2/24/7	0.921	17.78	12.56
	ANN_2	0.960	17.88	9.36
	ANN_2/24	0.964	12.04	8.63
	ANN_2/24/7	0.968	11.87	8.56
Adult education center	MLR_2	0.902	27.50	20.44
	MLR_2/24	0.917	25.37	18.43
	MLR_2/24/7	0.929	23.37	17.16
	ANN_2	0.937	15.87	14.62
	ANN_2/24	0.939	14.67	12.85
	ANN_2/24/7	0.967	11.57	9.54

7. Conclusions

This study analyzes the DH load patterns of a major city and five building types, identifies the main factors affecting load forecasting, proposes different models based on MLR and ANN, and compares their performances. A novel clustering method was developed to describe different DH load patterns and improve the accuracy of MLR. The conclusions are as follows:

(1) The DH load patterns of buildings and the city differed in *winter* (heating season) and *summer* (non-heating season), as well as according to the daily and weekly rhythms. The multiple linear dependencies between the DH load and outdoor temperature resulted from the different functions and operation modes of the buildings. Automation may lower the temperature and ventilation rate for some building types during nonworking hours.
(2) Including daily and weekly rhythms improved the forecasting accuracy of both the MLR and ANN methods for the city and building DH load forecasting. The improvements in forecasting accuracy caused by adding rhythms to different buildings differed because of the different DH load patterns that depend on how the building operates.
(3) The ANN methods provided more accurate DH load forecasts than the MLR methods for the buildings and city, regardless of whether the rhythms were considered. The ANN_2/24/7 model, with daily and weekly rhythms, exhibited optimal forecasting accuracy, with $R^2 > 0.93$, AMAPE 5.6 % for the city, and less than 10 % for the buildings, except for the Residential building. MLR methods are almost as effective at the city level and for buildings without strong nonlinear dependencies.
(4) When different operating modes cause nonlinearities, the novel clustering technique developed in this study can improve the

Table 10
Forecasting accuracy of different clusters using MLR_24/7.

Name	Models	RMSE (%)	AMAPE (%)
Mall	MLR_*winter*_1	10.0	6.9
	MLR_*winter*_2	8.4	6.3
	MLR_*winter*_3	13.0	9.7
	MLR_*winter*_4	10.8	8.4
	MLR_*summer*	31.0	22.2
	Total	12.8	9.1
Adult education center	MLR_*winter*_1	10.2	7.6
	MLR_*winter*_2	10.9	3.3
	MLR_*summer*	39.9	29.1
	Total	17.1	8.6

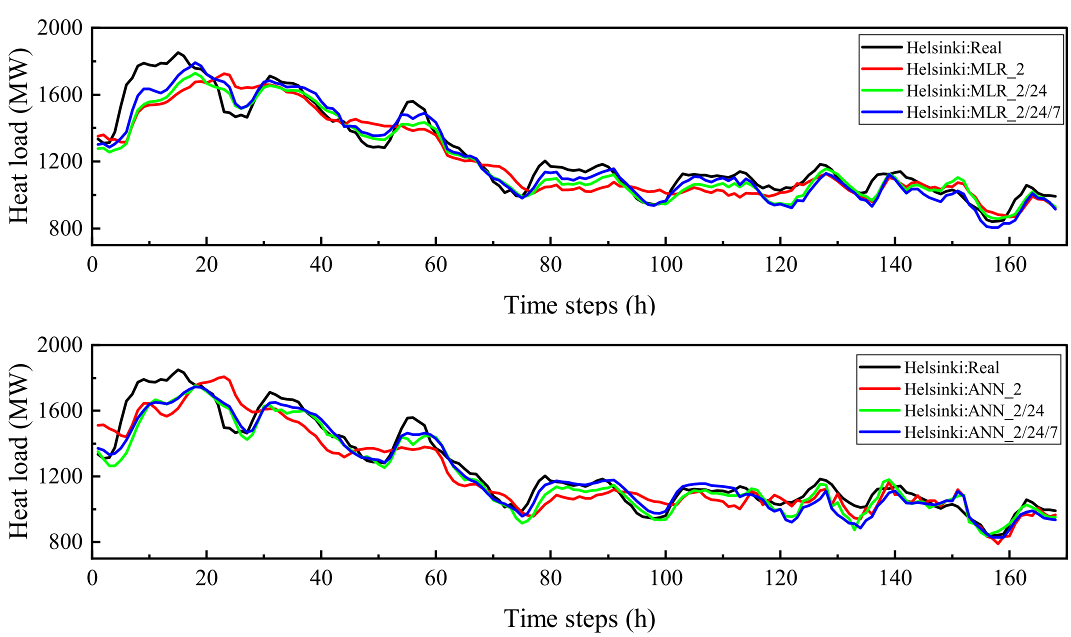

Fig. 7. Real and predicted data using six models for the city for a sample week from Monday to Sunday (February 22nd to 28th in 2021).

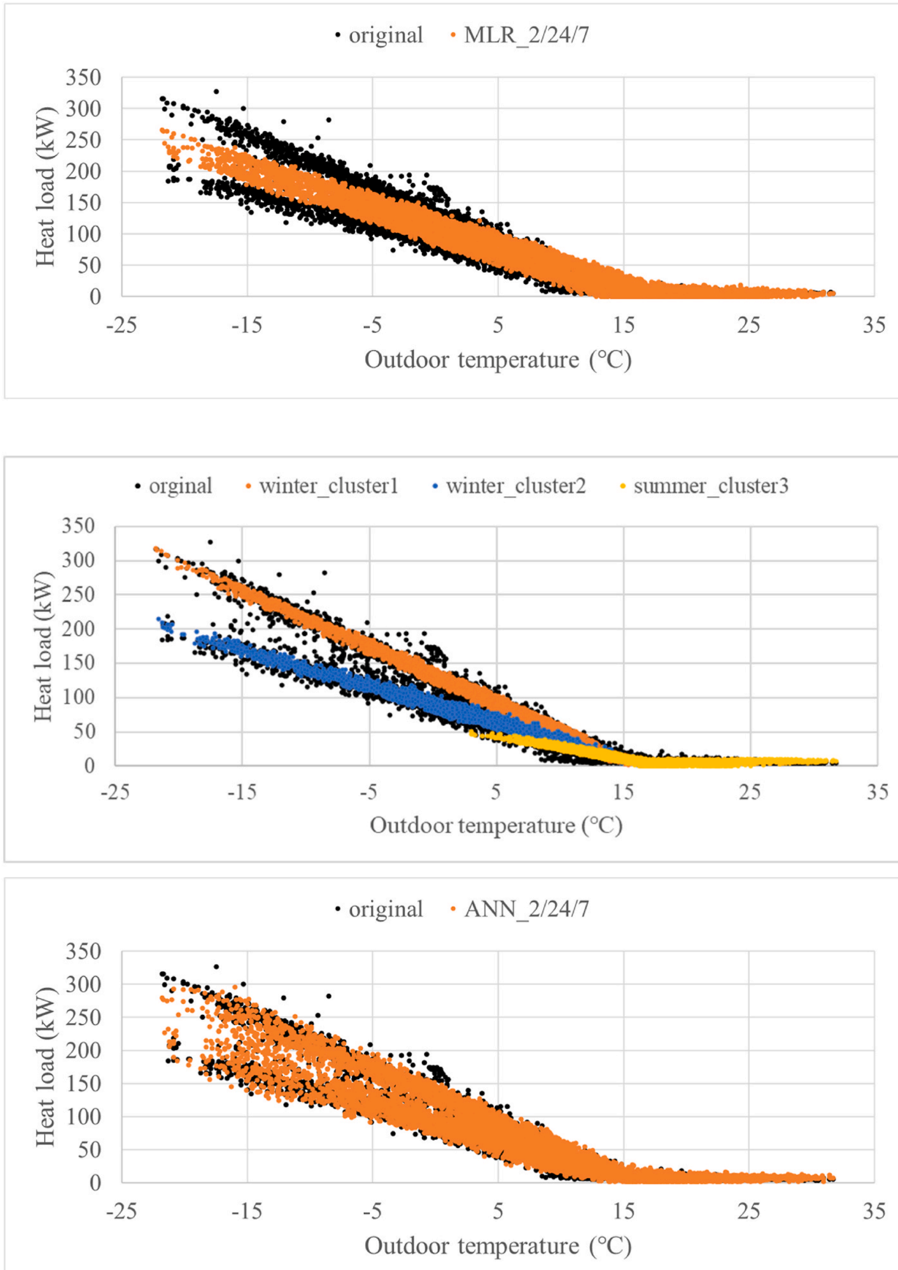

Fig. 8. Real and predicted data for the Adult education center. Top: MLR_2/24/7; middle: cluster-based MLR_24/7; bottom: ANN_2/24/7.

accuracy of the MLR forecasts to a level comparable to that of an ANN.

(5) The ANN_2/24/7 model has good application prospects for DH load forecasting in cities and buildings with DSM in the future. This is because the time-dependent indoor temperature control makes the DH load dependency nonlinear, which can be the best forecast by an ANN with daily and weekly rhythms. For example, an office building could control the indoor temperature at 20 °C during working hours and 16 °C during nights and weekends. To support the DSM for buildings, the improved accuracy caused by adding daily and weekly rhythms can be significant.

For DH load forecasting of buildings with nonlinear dependencies, ANN is superior to MLR; however, determining the hyperparameters of ANN is challenging for engineers who are not majoring in machine learning. Although MLR combined with a clustering method currently requires manual work, it is more effortless than determining suitable ANN hyperparameters. Engineers can use Excel to complete the heating load forecasting of the MLR combined clustering method without programming software. Another advantage of MLR with the clustering method is that the resulting clusters and obtained regression parameters have a straightforward interpretation that promotes an understanding of system behavior. In contrast, no such understanding is contributed by the ANN model. In future studies, we intend to improve the clustering method to achieve nonlinear decoupling for the heat load of buildings automatically. In addition, indoor temperature is essential in heat load forecasting at the building level. However, owing to the lack of measured indoor temperatures, these were not considered in this study. We will deploy temperature sensors in buildings and add indoor temperature as a factor in the MLR and ANN models to test the forecasting performance in our future studies.

CRediT authorship contribution statement

Pengmin Hua: Conceptualization, Formal analysis, Methodology, Software, Writing - original draft, Writing - review & editing. **Haichao Wang:** Funding acquisition, Writing - review & editing. **Zichan Xie:** Writing - review & editing. **Risto Lahdelma:** Formal analysis, Methodology, Supervision, Writing - review & editing.

Declaration of competing interest

The authors declare that they have no known competing financial interests or personal relationships that could have appeared to influence the work reported in this paper.

Data availability

Data will be made available on request.

Acknowledgements

This study was supported by the Academy Research Fellow project and allocated initial funding for research costs – Spatiotemporal dynamic simulation of the thermal energy storage (TES) assisted heating network and optimization for indoor temperature control (NO. 334205 and NO.336268). The authors would like to thank the Walter Ahlström Foundation for financially supporting this research (https://walterahlstrom.fi/).

References

[1] Kavvadias K, Jiménez-Navarro JP, Thomassen G. Decarbonising the EU heating sector - Integration of the power and heating sector, EUR 29772 EN. Publications Office of the European Union; 2019. https://doi.org/10.2760/943257. JRC114758.
[2] EASE. Thermal storage position paper. Ease 2017;1–13.
[3] Connolly D. Heat Roadmap Europe: quantitative comparison between the electricity, heating, and cooling sectors for different European countries. Energy 2017;139:580–93. https://doi.org/10.1016/j.energy.2017.07.037.
[4] Proposal for a Directive of the European Parliament and of the Council. Amending Directive 2012/27/EU. 2016. https://eur-lex.europa.eu/legal-content/EN/TXT/?uri=CELEX:52016PC0761.
[5] Lund H, Möller B, Mathiesen BV, Dyrelund A. The role of district heating in future renewable energy systems. Energy 2010;35:1381–90. https://doi.org/10.1016/j.energy.2009.11.023.
[6] Gorroño-Albizu L, de Godoy J. Getting fair institutional conditions for district heating consumers: insights from Denmark and Sweden. Energy 2021;237. https://doi.org/10.1016/j.energy.2021.121615.
[7] Gong M, Zhao Y, Sun J, Han C, Sun G, Yan B. Load forecasting of district heating system based on Informer. Energy 2022;253:124179. https://doi.org/10.1016/j.energy.2022.124179.
[8] Li X, Li W, Zhang R, Jiang T, Chen H, Li G. Collaborative scheduling and flexibility assessment of integrated electricity and district heating systems utilizing thermal inertia of district heating network and aggregated buildings. Appl Energy 2020;258:114021. https://doi.org/10.1016/j.apenergy.2019.114021.
[9] Zhao H, Wang B, Liu H, Sun H, Pan Z, Guo Q. Exploiting the flexibility inside park-level commercial buildings considering heat transfer time delay: a memory-augmented deep reinforcement learning approach. IEEE Trans Sustain Energy 2022;13:207–19. https://doi.org/10.1109/TSTE.2021.3107439.
[10] Guelpa E, Verda V. Demand response and other demand side management techniques for district heating: a review. Energy 2021;219:119440. https://doi.org/10.1016/j.energy.2020.119440.
[11] Egging-Bratseth R, Kauko H, Knudsen BR, Bakke SA, Ettayebi A, Haufe IR. Seasonal storage and demand side management in district heating systems with demand uncertainty. Appl Energy 2021;285:116392. https://doi.org/10.1016/j.apenergy.2020.116392.
[12] Guelpa E, Marincioni L, Deputato S, Capone M, Amelio S, Pochettino E, et al. Demand side management in district heating networks: a real application. Energy 2019;182:433–42. https://doi.org/10.1016/j.energy.2019.05.131.
[13] Runge J, Saloux E. A comparison of prediction and forecasting artificial intelligence models to estimate the future energy demand in a district heating system. Energy 2023;269:126661. https://doi.org/10.1016/j.energy.2023.126661.
[14] Sun Y, Haghighat F, Fung BCM. A review of the-state-of-the-art in data-driven approaches for building energy prediction. Energy Build 2020;221:110022. https://doi.org/10.1016/j.enbuild.2020.110022.
[15] Ding Y, Brattebø H, Nord N. A systematic approach for data analysis and prediction methods for annual energy profiles: an example for school buildings in Norway. Energy Build 2021;247:111160. https://doi.org/10.1016/j.enbuild.2021.111160.
[16] Ascione F, Bianco N, Mauro GM, Napolitano DF, Vanoli GP. Building heating demand vs climate: deep insights to achieve a novel heating stress index and climatic stress curves. J Clean Prod 2021;296:126616. https://doi.org/10.1016/j.jclepro.2021.126616.
[17] Magni M, Ochs F, de Vries S, Maccarini A, Sigg F. Detailed cross comparison of building energy simulation tools results using a reference office building as a case study. Energy Build 2021;250:111260. https://doi.org/10.1016/j.enbuild.2021.111260.
[18] Ghedamsi R, Settou N, Gouareh A, Khamouli A, Saifi N, Recioui B, et al. Modeling and forecasting energy consumption for residential buildings in Algeria using bottom-up approach. Energy Build 2016;121:309–17. https://doi.org/10.1016/j.enbuild.2015.12.030.
[19] Kristensen MH, Hedegaard RE, Petersen S. Long-term forecasting of hourly district heating loads in urban areas using hierarchical archetype modeling. Energy 2020;201. https://doi.org/10.1016/j.energy.2020.117687.
[20] Cui M. District heating load prediction algorithm based on bidirectional long short-term memory network model. Energy 2022;254:124283. https://doi.org/10.1016/j.energy.2022.124283.
[21] Fang T, Lahdelma R. Evaluation of a multiple linear regression model and SARIMA model in forecasting heat demand for district heating system. Appl Energy 2016;179:544–52. https://doi.org/10.1016/j.apenergy.2016.06.133.
[22] Ciulla G, D'Amico A. Building energy performance forecasting: a multiple linear regression approach. Appl Energy 2019;253:113500. https://doi.org/10.1016/j.apenergy.2019.113500.
[23] Niu D, Yu M, Sun L, Gao T, Wang K. Short-term multi-energy load forecasting for integrated energy systems based on CNN-BiGRU optimized by attention mechanism. Appl Energy 2022;313:118801. https://doi.org/10.1016/j.apenergy.2022.118801.
[24] Hu Y, Cheng X, Wang S, Chen J, Zhao T, Dai E. Times series forecasting for urban building energy consumption based on graph convolutional network. Appl Energy 2022;307:118231. https://doi.org/10.1016/j.apenergy.2021.118231.
[25] Koschwitz D, Frisch J, van Treeck C. Data-driven heating and cooling load predictions for non-residential buildings based on support vector machine regression and NARX Recurrent Neural Network: a comparative study on district scale. Energy 2018;165:134–42. https://doi.org/10.1016/j.energy.2018.09.068.
[26] Potočnik P, Škerl P, Govekar E. Machine-learning-based multi-step heat demand forecasting in a district heating system. Energy Build 2021;233. https://doi.org/10.1016/j.enbuild.2020.110673.
[27] Xue G, Qi C, Li H, Kong X, Song J. Heating load prediction based on attention long short term memory: a case study of Xingtai. Energy 2020;203:117846. https://doi.org/10.1016/j.energy.2020.117846.
[28] Bünning F, Heer P, Smith RS, Lygeros J. Improved day ahead heating demand forecasting by online correction methods. Energy Build 2020;211. https://doi.org/10.1016/j.enbuild.2020.109821.
[29] Wei Z, Zhang T, Yue B, Ding Y, Xiao R, Wang R, et al. Prediction of residential district heating load based on machine learning: a case study. Energy 2021;231:120950. https://doi.org/10.1016/j.energy.2021.120950.
[30] Lumbreras M, Garay-Martinez R, Arregi B, Martin-Escudero K, Diarce G, Raud M, et al. Data driven model for heat load prediction in buildings connected to District Heating by using smart heat meters. Energy 2022;239. https://doi.org/10.1016/j.energy.2021.122318.
[31] Pachauri N, Ahn CW. Weighted aggregated ensemble model for energy demand management of buildings. Energy 2023;263:125853. https://doi.org/10.1016/j.energy.2022.125853.
[32] Shakeel A, Chong D, Wang J. Load forecasting of district heating system based on improved FB-Prophet model. Energy 2023;278:127637. https://doi.org/10.1016/j.energy.2023.127637.
[33] Liu T, Tan Z, Xu C, Chen H, Li Z. Study on deep reinforcement learning techniques for building energy consumption forecasting. Energy Build 2020;208. https://doi.org/10.1016/j.enbuild.2019.109675.
[34] Xu Y, Li F, Asgari A. Prediction and optimization of heating and cooling loads in a residential building based on multi-layer perceptron neural network and different optimization algorithms. Energy 2022;240. https://doi.org/10.1016/j.energy.2021.122692.
[35] Wang Z, Liu X, Huang Y, Zhang P, Fu Y. A multivariate time series graph neural network for district heat load forecasting. Energy 2023;278:127911. https://doi.org/10.1016/j.energy.2023.127911.
[36] Lund H, Werner S, Wiltshire R, Svendsen S, Thorsen JE, Hvelplund F, et al. 4th Generation District Heating (4GDH). Integrating smart thermal grids into future sustainable energy systems. Energy 2014;68:1–11. https://doi.org/10.1016/j.energy.2014.02.089.
[37] Helen company official website. https://www.helen.fi/en/company/responsibility/current-topics/open-data. [Accessed 24 May 2022].
[38] Helsingin tilastotietokannat. https://kaupunkitieto.hel.fi/fi/helsingin-tilastotietokannat. [Accessed 25 April 2023].
[39] Finish meteorological institute official Website. https://en.ilmatieteenlaitos.fi/download-observations. [Accessed 24 May 2022].
[40] Energy Consumption Data of City of Helsinki's Utility and Service Properties. https://www.opendata.fi/data/en_GB/dataset/helsingin-kaupungin-palvelukiinteistojen-energiankulutustietoja. [Accessed 24 May 2022].
[41] Zhang L, Li J, Xu X, Liu F, Guo Y, Yang Z, et al. High spatial granularity residential heating load forecast based on Dendrite net model. Energy 2023;269:126787. https://doi.org/10.1016/j.energy.2023.126787.

[42] Cengel YA. Heat transference a practical approach, vol. 4. MacGraw-Hill; 2004. p. 874.
[43] Han J-C. Analytical heat transfer. 2008.
[44] Wang J. Sports performance prediction model based on BP neural network application research. Biotechnol An Indian J 2014;10:2933–9.
[45] Hyndman RJ, Athanasopoulos G. Forecasting: principles and practice. OTexts; 2018.
[46] Salem H, Kabeel AE, El-Said EMS, Elzeki OM. Predictive modelling for solar power-driven hybrid desalination system using artificial neural network regression with Adam optimization. Desalination 2022;522:115411. https://doi.org/10.1016/j.desal.2021.115411.
[47] Walls S, Binns AD, Levison J, MacRitchie S. Prediction of actual evapotranspiration by artificial neural network models using data from a Bowen ratio energy balance station. Neural Comput Appl 2020;32:14001–18. https://doi.org/10.1007/s00521-020-04800-2.